

## Nonlinear Generation of Vorticity by Surface Waves

S. V. Filatov,<sup>1</sup> V. M. Parfenyev,<sup>2,3,\*</sup> S. S. Vergeles,<sup>2,3</sup> M. Yu. Brazhnikov,<sup>1</sup> A. A. Levchenko,<sup>1</sup> and V. V. Lebedev<sup>2,3</sup>

<sup>1</sup>*Institute of Solid State Physics, Chernogolovka, 2 Academician Ossipyan str., 142432 Moscow Region, Russia*

<sup>2</sup>*Landau Institute for Theoretical Physics, Chernogolovka, 1-A Akademika Semenova av., 142432 Moscow Region, Russia*

<sup>3</sup>*Moscow Institute of Physics and Technology, Dolgoprudny, 9 Institutskiy per., 141700 Moscow Region, Russia*

(Received 8 June 2015; published 5 February 2016)

We demonstrate that waves excited on a fluid surface produce local surface rotation owing to hydrodynamic nonlinearity. We examine theoretically the effect and obtain an explicit formula for the vertical vorticity in terms of the surface elevation. Our theoretical predictions are confirmed by measurements of surface motion in a cell with water where surface waves are excited by vertical and harmonic shaking the cell. The experimental data are in good agreement with the theoretical predictions. We discuss physical consequences of the effect.

DOI: 10.1103/PhysRevLett.116.054501

Waves excited on the fluid surface are well described in terms of the potential fluid motion. The approximation is justified by the weakness of the wave damping. In this case, the fluid vorticity is expected to be nonzero in a narrow layer near the fluid surface where viscosity is relevant [1,2]. In the linear approximation the vorticity is directed along the unperturbed fluid surface; therefore, its vertical component is zero and yet the solenoidal motion of the fluid surface generated by surface waves was recently observed; see Refs. [3–5]. The waves were excited due to Faraday instability [1,6] and were sufficiently strong to produce intense solenoidal surface currents.

However, the generation mechanism of the solenoidal currents from the surface waves remained so far obscure. We show that the mechanism is related to nonlinearity of surface waves. One can roughly say that the surface tilt produces a tilt of the vorticity in the viscous sublayer as well. A first-ever theory explaining the generation of surface solenoidal motion by surface waves is developed and quantitative predictions are made. For the simplest case of two plane surface waves the theory was checked experimentally.

We demonstrate that surface waves of close frequencies can generate surface solenoidal currents varying slowly in time and varying in space on the wavelength scale. It turns out that the velocity associated with the currents can be estimated as  $v^2k/\omega$ , where  $v$  is the surface velocity in the generated waves,  $k$  is their wave vector, and  $\omega$  is their frequency. Surprisingly, the expression for the velocity is independent of viscosity though it is produced by the viscous mechanism. This property can be compared to hydrodynamic turbulence. Its characteristics in the inertial interval of scales are independent of viscosity although it is viscous dissipation that ensures the statistical stationarity.

Let us present our theoretical scheme. The bulk motion of an incompressible fluid is described by the Navier-Stokes equation [1,2]

$$\partial_t \mathbf{v} + (\mathbf{v} \nabla) \mathbf{v} = -\nabla P / \rho + \nu \nabla^2 \mathbf{v}, \quad (1)$$

where  $\rho$  and  $\nu$  are the fluid mass density and the kinematic viscosity coefficient, respectively,  $\mathbf{v}$  is the fluid velocity and  $P$  is pressure. Equation (1) has to be supplemented by the incompressibility condition  $\text{div } \mathbf{v} = 0$ . The equation for the vorticity,  $\boldsymbol{\omega} = \text{curl } \mathbf{v}$ , is

$$\partial_t \boldsymbol{\omega} = -(\mathbf{v} \nabla) \boldsymbol{\omega} + (\boldsymbol{\omega} \nabla) \mathbf{v} + \nu \nabla^2 \boldsymbol{\omega}. \quad (2)$$

The Navier-Stokes equation (1) has to be supplemented by the boundary conditions at the fluid surface. First it is the kinematic boundary condition [1]

$$\partial_t h = v_z - v_x \partial_x h - v_y \partial_y h, \quad (3)$$

implying that the fluid surface moves with the fluid velocity  $\mathbf{v}$ . Here and thereafter we assume that the axis  $Z$  is directed vertically, opposite to the gravitational acceleration  $\mathbf{g}$  and that the equilibrium fluid surface coincides with plane  $z = 0$ . The deviations from the equilibrium shape are described by the elevation  $h(t, x, y)$ .

There is also the dynamic boundary condition that can be obtained from the requirement of zero momentum flux through the fluid surface [1,2]. This leads to the conditions

$$P - 2\rho\nu n_i n_k \partial_i v_k = \rho gh + \sigma(\nabla \mathbf{n}), \quad (4)$$

$$(\delta_{ij} - n_i n_j) n_k (\partial_j v_k + \partial_k v_j) = 0, \quad (5)$$

to be satisfied at  $z = h$ . Here,  $\sigma$  is the surface tension coefficient and  $\mathbf{n}(t, x, y) = (-\partial_x h, -\partial_y h, 1) / \sqrt{1 + (\nabla h)^2}$  is the unit vector normal to the surface. The boundary condition for the vorticity  $\boldsymbol{\omega}_i = \epsilon_{ijk} \partial_j v_k$  follows from Eq. (5)

$$n_m n_k \partial_k \boldsymbol{\omega}_m + (\partial_i v_k + \partial_k v_i) \epsilon_{imn} n_m K_{kn} = 0, \quad (6)$$

where  $\epsilon_{ijk}$  is the unit antisymmetric tensor and we introduced the curvature tensor  $K_{ik} = K_{ki} = (\delta_{ij} - n_i n_j) \partial_j n_k$ .

Further we consider the case where some waves are excited on the fluid surface. The case of deep water is implied. We assume that the wave steepness is small, i.e.,  $|\nabla h| \ll 1$ . In the linear approximation we deal with the gravitational-capillary waves characterized by the dispersion law  $\omega^2 = gk + (\sigma/\rho)k^3$ , where  $k$  is wave vector of the wave and  $\omega$  is its frequency. We also assume that the waves are weakly decaying, i.e.,  $\gamma = \sqrt{\nu k^2/\omega} \ll 1$ .

In the linear approximation, all the quantities characterizing the surface waves can be expressed via the surface elevation  $h$ . The explicit expressions for the velocity and the vorticity in the leading order with respect to the small parameter  $\gamma$  are

$$v_\alpha = \nu[(\hat{\kappa}^2 + \hat{k}^2)/\hat{k}] \exp(\hat{k}z) \partial_\alpha h - 2\nu\hat{k} \exp(\hat{k}z) \partial_\alpha h, \quad (7)$$

$$v_z = \nu(\hat{\kappa}^2 + \hat{k}^2) \exp(\hat{k}z) h - 2\nu\hat{k}^2 \exp(\hat{k}z) h, \quad (8)$$

$$\varpi_\alpha = 2\epsilon_{\alpha\beta} \exp(\hat{k}z) \partial_\beta \partial_t h, \quad (9)$$

see, e.g., Ref. [1]. Here and below Greek indices run over  $x, y$ ,  $\epsilon_{\alpha\beta}$  is the unit antisymmetric tensor and we introduced the nonlocal operators  $\hat{\kappa} = (-\partial_x^2 - \partial_y^2)^{1/2}$ ,  $\hat{k} = (\partial_t/\nu + \hat{\kappa}^2)^{1/2}$ . The first terms in the expressions (7), (8) correspond to the potential part of the velocity, whereas the last terms represent corrections, arising due to viscosity. Note that the vorticity  $\varpi_\alpha$  is located in a relatively thin layer near the surface. The depth of the layer is estimated as  $\gamma/k \ll 1/k$ , where  $1/k$  is the penetration depth of the potential part of the velocity.

The  $Z$  component of the vorticity  $\varpi_z$  is zero in the linear approximation, it appears only due to the nonlinear wave interaction. Therefore, to find  $\varpi_z$  one should go beyond the approximation. We take into account the main nonlinear contribution to  $\varpi_z$  in Eq. (2), which is of the second order in the wave amplitude:

$$(\partial_z^2 - \hat{\kappa}^2) \varpi_z = -\nu^{-1} \varpi_\alpha \partial_\alpha v_z. \quad (10)$$

The term on the right-hand side can be regarded as a source with respect to  $\varpi_z$ . It corresponds to the rotation of two-dimensional vector  $\varpi_\alpha$  by the velocity field of the surface waves. We keep the nonlinear terms of the same order in the boundary condition (6):

$$\partial_z \varpi_z = \partial_\alpha h \partial_z \varpi_\alpha - \epsilon_{\alpha\gamma} (\partial_\alpha v_\beta + \partial_\beta v_\alpha) \partial_\beta \partial_\gamma h. \quad (11)$$

Note that the second term on the right-hand side of Eq. (11) is smaller than the first one in parameter  $\gamma$ . However, the second term should be kept since it may give a comparable contribution to the surface value of  $\varpi_z$ , because it can produce a correction which has longer penetration depth; see Ref. [7].

The solution of Eq. (10) with the boundary conditions (11) (which can be posed at  $z=0$ ) and  $\varpi_z \rightarrow 0$  at  $z \rightarrow -\infty$  is

$$\begin{aligned} \varpi_z(z) = & 2\epsilon_{\alpha\beta} (e^{\hat{k}z} \partial_\alpha h) (e^{\hat{k}z} \partial_\beta \partial_t h) \\ & + 2\epsilon_{\alpha\beta} \hat{\kappa}^{-1} e^{\hat{k}z} (\partial_\alpha h \partial_\beta \partial_t \hat{k} h + \partial_\alpha \partial_\gamma h \partial_\beta \partial_\gamma \partial_t \hat{k}^{-1} h), \end{aligned} \quad (12)$$

where Eqs. (7)–(9) were used. The surface value of the vorticity  $\varpi_z$  is obtained by substituting  $z=0$  into the expression (12). The first term in the expression (12) represents the tilt of the vorticity (9) due to the surface tilt. The first term in the last round brackets is the result of spreading of rotated vorticity into the bulk. The last term in the expression (12) is related to the nonzero curvature of the surface, which gives rise to an additional viscous tangential surface force.

Note that, according to Eq. (12), a single surface plane wave does not produce  $\varpi_z$ , nonzero  $\varpi_z$  arises if at least two plane waves propagating in different directions are excited. The characteristic frequency  $\omega_v$  of vorticity  $\varpi_z$  can vary from zero to the order of the surface wave frequency  $\omega$ , since we consider the nonlinearity of the second order. If  $\omega_v \gg \nu k^2$  then the first term on the right-hand side of Eq. (12) is leading. Otherwise, both terms are of the same order.

Further, we analyze the case when the excited surface waves are characterized by a narrow spectrum peaked near  $\omega$  with the width  $\Delta\omega \ll \omega$ . Then the slowly varying contribution into the vertical vorticity  $\varpi_z$  is leading and thus  $\omega_v \sim \Delta\omega$ . Indeed, from Eq. (12) it follows that the relative amplitude of double-frequency contribution is small as  $\Delta\omega/\omega$ ; see Ref. [7]. Next, we assume  $\omega_v \ll \nu k^2$ . In this case one can substitute  $\hat{\kappa}$  by  $\hat{k}$  in the second line of Eq. (12). So, the first term on the right-hand side of Eq. (12) is localized on the scale  $\gamma/k$  near the surface, while the second term penetrates deeper, on distance  $1/k$ . Both terms have comparable magnitudes at the surface.

Let us formulate the applicability conditions for our theory that is correct if the higher-order nonlinear terms are small compared to the kept ones. We have to estimate the nonlinear terms from Eq. (2) where the second-order terms for the velocity,  $v^{(2)}$ , have to be taken into account. From Eq. (12) it follows that  $v^{(2)} \sim \omega k h^2$ . Therefore, the nonlinear terms with  $v^{(2)}$  are small if  $(v^{(2)} \nabla) \varpi_z \ll \nu \Delta \varpi_z$ . Thus, in the case  $\omega_v \lesssim \nu k^2$  we arrive at the condition  $kh \ll \gamma$ , which is stronger than the small steepness condition  $kh \ll 1$ . The condition can be rewritten also as  $\kappa h \ll 1$ .

Now we turn to the experimental part. To check the theoretical predictions, we carried out experiments with a rectangular cell filled with water. Surface waves were excited in the cell by its shaking. The experimental setup for measurements of the water surface motion are shown in Fig. 1(a). The vessel, shaped as nearly square with sides from 40 to 50 mm and depth of 10 mm, is filled with distilled water and is set horizontally with an accuracy of 1.5 degrees. The water level is adjusted to form concave or convex meniscus on the walls, Fig. 1(b). The vessel was fixed on a platform performing harmonic oscillations with cyclic frequency  $\omega$  in the vertical direction. The oscillation amplitude and frequency were specified by a computer-controlled

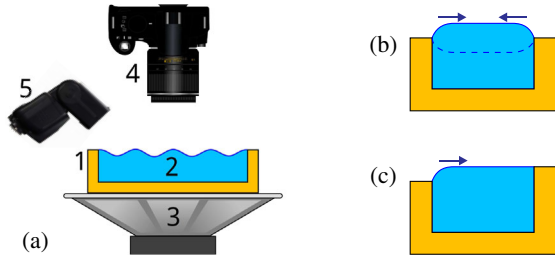


FIG. 1. Experimental setup for registration of the water surface motion. (a) The scheme of the setup: 1, vessel; 2, water; 3, vibroplatform; 4, photo camera; 5, flashlight. (b) Concave or convex meniscus is formed on the edge of walls depending on amount of water used to fill the vessel. (c) Configuration of water meniscus in square cell, which has walls of different height designed to suppress generation of waves from a pair of adjacent walls. Arrows show the direction of wave propagation.

external digital-to-analog converter. The acceleration was measured by an accelerometer fixed on the vibroplatform. The exciting frequency  $\omega/2\pi$  in the range from 40 to 60 Hz was in resonance with one of the surface eigenmodes of the water in the vessel. The oscillation amplitude was smaller than the threshold of the Faraday instability [1,6].

To visualize the surface motion, hollow glass spheres from 10 to 30 mm in diameter were poured on the water surface. The average density of the glass spheres was insignificantly less than the water density. The slow motion of particles was captured by a camera that took sequential pictures of the water surface upon illumination. Then the video of the slow surface motion was built from sequential frames. The photographs were processed by the MatLab program and the velocity field was built using the PIVlab software package [8], then the vorticity was calculated in accordance with the relation  $\varpi_z = \partial_x v_y - \partial_y v_x$ .

A stationary pattern of standing capillary ripples is formed within 1–2 s after turning on the excitation. Simultaneously with the ripples, a square lattice of vortices on the water surface originates. The whole picture remains stable at least for several minutes. The results of the experimental procedure are presented in Figs. 2 and 4 showing the vorticity  $\varpi_z$  averaged over time. The red color corresponds to positive vorticity, the blue color corresponds to negative vorticity, and the color scale determining the vorticity value is also presented in the figures.

To explain the pictures, let us first note that the forces exciting the waves are related to the water meniscus formed near the walls. Therefore, the forces are localized near the walls and free hydrodynamic equations can be used to describe the water motion not very close to the walls. One deals with nearly linear waves of a given frequency, the amplitude of the waves is determined by the near-wall forces and boundary conditions. Only waves propagating perpendicular to the walls of the rectangular vessel are excited. The resonant frequencies correspond to the waves which wavelengths satisfy the condition for resonance: the

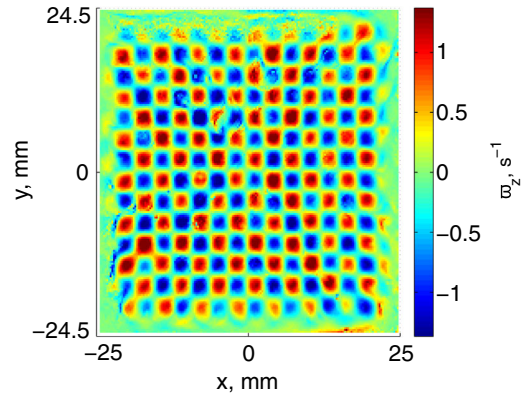


FIG. 2. Vorticity in a cell  $50 \times 49 \text{ mm}^2$  where the surface waves with frequency 42.7 Hz are excited. The observed chess-like pattern of the vorticity field is consistent with the theoretical expression (14), the periods of the pattern in the  $X$  and  $Y$  directions are equal to the wavelength.

length of the vessel wall is equal to an integer number of wavelengths up to some correction associated with the near-wall area. The linear size of the vessels is small enough so that the distance in frequency domain between neighboring resonances is greater than the width of the resonances. The waves propagating in different directions are not excited since the power transferred from the meniscus to the waves is zero in this case.

Figure 2 represents the vorticity observed in a nearly square cell where the standing waves are excited in the  $X$  and  $Y$  directions. Neglecting the wave damping, we can model the elevation as

$$h = H_1 \cos(\omega t) \cos(kx) + H_2 \cos(\omega t + \psi) \cos(ky), \quad (13)$$

where  $k$  is determined by the dispersion law. The phase shift  $\psi$  in Eq. (13) is related to the cell asymmetry, that leads to different boundary conditions for the standing waves in the  $X$  and  $Y$  directions. Changing the aspect ratio of the cell one can affect the phase shift  $\psi$ . Substituting the expression (13) into Eq. (12) we obtain

$$\varpi_z(0) = -(2 + \sqrt{2}) \sin \psi H_1 H_2 \omega k^2 \sin(kx) \sin(ky). \quad (14)$$

The result is time independent. The sum of the rational and irrational numbers corresponds to the sum of the two terms in Eq. (12), which have different penetration depths. The expression (14) is in a qualitative agreement with Fig. 2.

We also conducted experiments with a square cell, where the phase shift  $\psi \ll 1$  and the vorticity distribution changes significantly. To describe the situation one should take into account the wave attenuation along the direction of wave propagation due to the viscous damping. Details are presented in the Supplemental Material [7].

The magnitude of the vorticity as a function of the wave amplitude is plotted in Fig. 3. The surface elevation caused

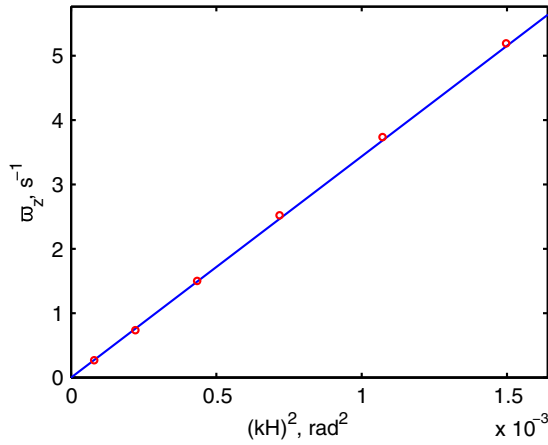


FIG. 3. Vorticity for different pumping amplitudes in a cell  $50 \times 49 \text{ mm}^2$ , where surface waves with frequency 42.7 Hz are excited, plotted as a function of the tilt amplitude  $kH$ . The line corresponds to the dependence  $\varpi_z \propto (kH)^2$  and it proves that the vorticity is generated by the second-order nonlinearity.

by the waves was measured by the laser beam reflected from the fluid surface. The size of laser projection on a screen can be recalculated into the surface tilt amplitude  $kH$ , where  $H$  is the amplitude of the largest wave. The graph in Fig. 3 demonstrates the square dependence of vorticity on the tilt amplitude, in accordance with our theoretical expectations.

Figure 4 presents results of another experiment. In this case the square vessel has walls of different height: two adjacent walls are slightly lower than two opposite walls. The vessel is filled with water exactly up to the edge of the higher walls to avoid menisci there. On the lower walls water forms a convex meniscus [see Fig. 1(c)]. Thus the exciting forces are applied to the water solely at the lower walls. Neglecting the effect of reflected waves, one can roughly model the situation by running waves propagating from low walls. Then the elevation is modeled as

$$h = H_1 \cos(\omega t - kx) + H_2 \cos(\omega t - ky). \quad (15)$$

Substituting the expression (15) into Eq. (12) one finds

$$\varpi_z(0) = -(2 + \sqrt{2})H_1H_2\omega k^2 \sin(kx - ky). \quad (16)$$

Note that the result is also time independent. Figure 4 demonstrates that the spatial wave damping is relevant. An account of the damping corrects the expression (16), that leads to a reasonable agreement between the experimental data and the theoretical predictions [7].

To conclude, we have discovered a new mechanism of surface vorticity generation related to the narrow viscous layer formed by propagating surface waves. In particular, this mechanism leads to surface mixing that can be characterized by the diffusion coefficient  $D$  that is of the fourth order in the wave amplitude, as for the direct action

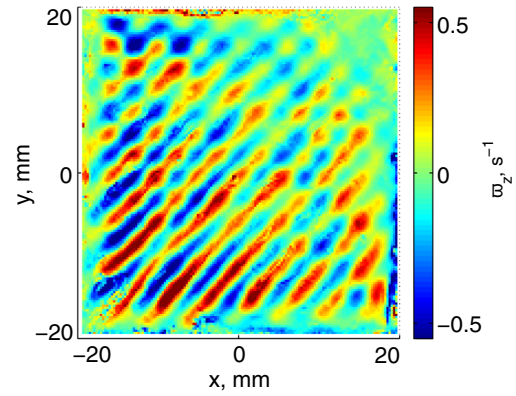


FIG. 4. Vorticity in a cell  $40 \times 40 \text{ mm}^2$ , where surface waves with frequency 54 Hz are excited. Two walls of the cell, corresponding to the left and bottom sides in the figure, are slightly lower than the other walls. The water level is adjusted to produce mainly two running waves from the lower walls, Fig. 1(c). Alternating stripes of positive and negative vorticity directed parallel to the diagonal of the square cell is in agreement with the theoretical expression (16).

of the waves on the fluid surface [9,10]. The problem requires further research.

Although the experiments were performed in the capillary range, our theoretical scheme is equally applicable to the gravitational range. For instance, the suggested theory can be used to analyze the solenoidal motion on the ocean surface.

Increasing an amplitude of the cell shaking one can reach threshold for the Faraday instability. Well above the threshold, the surface waves are quite intensive, which results in intense solenoidal motions of the fluid surface, for which the dimensionless parameter  $kh \gtrsim 1$ . Then the self-interaction of solenoidal motions becomes relevant [11], which leads, in particular, to the formation of an inverse energy cascade [4]. The results of our theoretical and experimental studies allow one to better understand the phenomenon and to develop a quantitative framework for it.

We are grateful to I. Kolokolov for valuable discussions. This work was supported by the Russian Scientific Foundation, Grant No. 14-22-00259.

\*parfenius@gmail.com

- [1] H. Lamb, *Hydrodynamics*, 6th ed. (Cambridge University Press, Cambridge, England, 1975).
- [2] L. D. Landau and E. M. Lifshitz, *Course of Theoretical Physics*, Vol. 6, Fluid Mechanics, 2nd English ed., (Pergamon Press, Oxford, England, 1987).
- [3] A. von Kameke, F. Huhn, G. Fernandez-Garcia, A. P. Munuzuri, and V. Perez-Munuzuri, *Phys. Rev. Lett.* **107**, 074502 (2011).
- [4] N. Francois, H. Xia, H. Punzmann, and M. Shats, *Phys. Rev. Lett.* **110**, 194501 (2013).

- [5] N. Francois, H. Xia, H. Punzmann, S. Ramsden, and M. Shats, *Phys. Rev. X* **4**, 021021 (2014).
- [6] M. Faraday, *Phil. Trans. R. Soc. London* **121**, 299 (1831).
- [7] See Supplemental Material at <http://link.aps.org/supplemental/10.1103/PhysRevLett.116.054501> for details of the calculations.
- [8] W. Thielicke and E. J. Stamhuis, *J. Open Res. Software* **2**, e30 (2014).
- [9] G. Falkovich, *J. Fluid Mech.* **638**, 1 (2009).
- [10] O. Bühler and M. Holmes-Cerfon, *J. Fluid Mech.* **638**, 5 (2009).
- [11] H. Punzmann, N. Francois, H. Xia, G. Falkovich, and M. Shats, *Nat. Phys.* **10**, 658 (2014).